



# Turbulent viscosity measurements relevant to planetary core-mantle dynamics

Daniel Brito<sup>a,\*</sup>, Jonathan Aurnou<sup>b,1</sup>, Philippe Cardin<sup>a</sup>

<sup>a</sup> *LGIT, Observatoire des Sciences de l'Univers de Grenoble, Grenoble, France*

<sup>b</sup> *Department of Terrestrial Magnetism, Carnegie Institution of Washington, Washington, USA*

Received 21 February 2003; received in revised form 25 July 2003; accepted 4 August 2003

## Abstract

Laboratory experiments that combine thermal convection in a rapidly rotating shell with a sudden increase of the shell's rotation rate (spin-up) enable us to study processes related to turbulent viscous coupling between planetary fluid cores and solid mantles. We experimentally measure the large-scale effective viscosity by determining how the synchronisation time between the fluid and the shell (called the spin-up time) is shortened when convective turbulence exists in the bulk of the fluid. Our experiments suggest that viscous core-mantle coupling in planets may be greater than has been previously estimated using molecular viscosity values.

© 2003 Elsevier B.V. All rights reserved.

*Keywords:* Planetary cores; Core-mantle interaction; Turbulent viscosity; Geodynamo

## 1. Introduction

Ludwig Prandtl (1925), modelling the turbulent flow produced by an obstacle, employed an effective fluid viscosity (Frish, 1995) that was greater than the molecular viscosity. In contrast to molecular viscosity, which describes a fluid's molecular transport of momentum, the concept of turbulent viscosity also takes into account the turbulent transport by regarding small scale turbulent eddies as “macro-molecules”. In some cases the turbulent viscosity may be modelled by an additional term in the equation of motion,  $\nu_t \Delta u$  here  $\nu_t$  is the turbulent viscosity coefficient,

$\Delta$  the Laplacian operator and  $u$  the velocity field. In this simple parameterisation, the turbulent viscosity appears to be a property of the fluid itself. This is not correct. Instead, the increase in effective viscosity results from enhanced momentum transfer by turbulence within the flow field. Therefore, the turbulent viscosity is a property of the flow and depends upon the details of the flow field. It may be understood as a mean contribution of the Reynolds stress term (Frish, 1995) that is derived from the non-linear  $u \cdot \nabla u$  term in the Navier–Stokes equation.

In geophysical fluid dynamics, this concept of turbulent viscosity is often used to explain measurements of the viscous boundary layers (known as Ekman boundary layers) that form in rotating, turbulent flows (Pedlosky, 1987). For example, the predicted thickness of the oceanic Ekman boundary layer is approximately 10 cm using molecular viscosity values whereas in situ measurements require a much larger

\* Corresponding author. Tel.: +33-476-82-80-42; fax: +33-476-82-81-01.

E-mail address: [daniel.brito@ujf-grenoble.fr](mailto:daniel.brito@ujf-grenoble.fr) (D. Brito).

<sup>1</sup> Present address: Department of Earth and Space Sciences, UCLA, USA.

effective fluid viscosity to explain the actual thickness of 10–100 m. Throughout this paper we will use the concept of turbulent viscosity to explain processes within the Ekman boundary layer that develops between our experiment's rotating shell and the fluid.

When modelling planetary core processes, it is crucial to estimate the effective viscosity of turbulent core fluids. In the deep Earth, the molecular viscosity of pure iron at core conditions (Poirier, 1988) is deduced from ab initio numerical simulations (De Wijs et al., 1998) as well as laboratory measurements (Dobson et al., 2000; Rutter et al., 2002) to have an approximate value  $\nu \sim 10^{-6} \text{ m}^2/\text{s}$ . On the other hand, a large-scale effective viscosity of  $10^{-1} \text{ m}^2/\text{s}$  is required to explain geodetic observations of Earth's nutations in terms of a viscous torque at the core-mantle boundary (Buffett, 1992). Ultimately, the published viscosity estimates of the Earth's outer core fluid (Secco, 1995) show an even more extreme range of values (up to  $10^6 \text{ m}^2/\text{s}$  in Smylie (1999)).

The strength of viscous forces in rotating systems is measured by the Ekman number,  $E = \nu/\Omega R^2$ , where  $\nu$  is the fluid viscosity,  $\Omega$  the angular rotation rate and  $R$  the spherical radius. Based on the molecular viscosity of iron,  $E$  is between  $10^{-12}$  and  $10^{-15}$  in terrestrial planetary cores. At present, geodynamo simulations (Glatzmaier and Roberts, 1995; Kuang and Bloxham, 1997; Olson et al., 1999; Jones, 2000; Glatzmaier, 2002) are carried out using  $E$  values no lower than  $10^{-5}$ , i.e. using very high viscosity values. Yet, strikingly common features exist between the numerical

results at large Ekman numbers (Olson et al., 1999) and the geomagnetic observations (Hulot et al., 2002). This has led to the argument (Glatzmaier and Roberts, 1995; Kuang and Bloxham, 1997; Jones, 2000) that large-scale core dynamics are controlled by a turbulent, effective viscosity that is far greater than molecular estimates, analogous to the findings of oceanic and atmospheric studies. Here, for the first time, we give experimental evidence for the existence of turbulent viscosity in a fluid mechanical experiment relevant to Ekman boundary layer dynamics and core-mantle coupling in planetary cores.

## 2. Experimental set-up

Following the ideas of Busse and Carrigan (1976), Cardin and Olson (1994) and Sumita and Olson (1999), the experimental device has been built to study thermal convection in a rapidly rotating shell (Aubert et al., 2001) that models core dynamics in planets. The experimental set-up is composed of a Plexiglas sphere (radius  $R_2 = 110 \text{ mm}$ ) and a cylinder (radius  $R_1 = 40 \text{ mm}$ ) that are both concentric with the rotation axis (see Fig. 1). The device spins at an angular rotation rate,  $\Omega$ , which can reach 600 rpm (revolutions per min). Temperatures  $T_1$  and  $T_2$  of the cylinder and the outer sphere, respectively, are monitored during experiments with a precision of 0.1 K. Thermal convection develops in the shell when the Rayleigh number,  $Ra$ , becomes greater than its

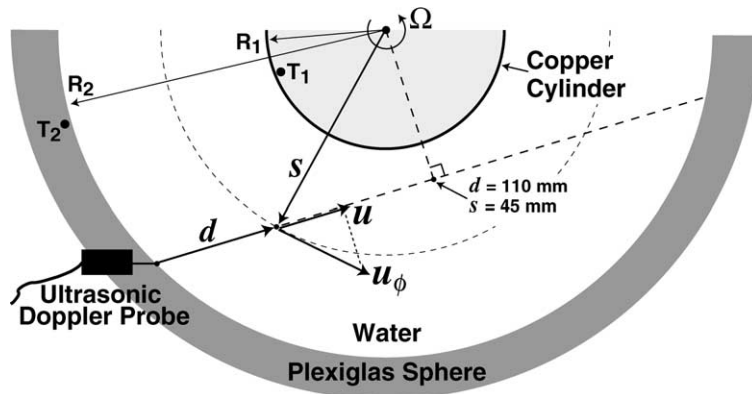


Fig. 1. Schematic top view onto the equatorial plane of one half of the experimental device. And  $d$  is the distance relative to the origin of the velocity profile from the probe,  $s$  the cylindrical radius in the equatorial plane. Temperatures are measured at  $T_1$  and  $T_2$  with platinum thermo-resistive probes in the copper cylinder and in the Plexiglas shell, respectively.

critical value,  $Ra_C$ . Here, the Rayleigh number is defined as  $Ra = \alpha \Delta T \Omega^2 D^4 / (\nu \kappa)$  where  $\alpha$  is the thermal expansion coefficient,  $\Delta T = (T_2 - T_1)$  is the temperature difference across the shell,  $D = (R_2 - R_1)$  is the shell thickness, and  $\kappa$  is the thermal diffusivity. For ratios  $Ra/Ra_C > 5$  convection becomes turbulent (Busse and Carrigan, 1976; Cardin and Olson, 1994; Sumita and Olson, 1999; Aubert et al., 2001). Convection occurs in the range  $20 \leq Ra/Ra_C \leq 80$  in the experiments presented here.

### 3. Velocity measurements during spin-up

The set-up also consists of an ultrasonic Doppler velocimetry system (Brito et al., 2001), used to quantitatively measure fluid velocities within the shell. A 4 MHz ultrasonic probe measures the velocity  $u$  along the ultrasonic beam in the equatorial plane of the rotating sphere (shown as the continuous line in Fig. 1). The spatial-resolution of the velocity measurements is  $\sim 0.5$  mm and profiles are registered every 43 ms.

A well-developed linear theory exists (Greenspan, 1969) to describe the hydrodynamics of the flow following the spin-up of a rotating, axisymmetric container of fluid. After a sudden change of rotation rate,  $\Delta\Omega$ , of a container initially rotating at  $\Omega$ , viscous Ekman boundary layers form along the walls of the container. Strong viscous effects spin-up the fluid within the Ekman layers to the new rotation rate of the container. Meanwhile, the unperturbed interior flow remains geostrophic, meaning that the flow field remains nearly two-dimensional, with little variation along the direction of the rotation axis (Greenspan, 1969; Busse and Carrigan, 1976; Pedlosky, 1987). The mismatch in the vorticity field across the Ekman layer induces a secondary flow, known as Ekman suction. Ekman suction pulls fluid from the interior into the Ekman layer where it is spun-up. This re-equilibration occurs as an exponential process with a characteristic spin-up time-scale,  $\tau$ , that scales as  $E^{-1/2}\Omega^{-1}$  which, in turn, scales with the fluid viscosity as  $\nu^{-1/2}$ . Because the interior flow remains geostrophic, spin-up also depends on the local height of fluid columns aligned parallel to the rotation axis. The longer the column, the longer it takes for Ekman suction to cycle the column's fluid through the Ekman layer. Therefore, in a sphere of radius  $R$ , the spin-up time decreases with increasing

cylindrical radius,  $s$ , and the azimuthal velocity,  $u_\phi$ , measured on a Doppler probe situated in the rotating reference frame, varies as

$$\begin{aligned} u_\phi(s, t) &= -s \Delta\Omega \exp\left[-\frac{t}{E^{-1/2}\Omega^{-1}(1-s^2/R^2)^{3/4}}\right] \\ &= -s \Delta\Omega \exp\left[-\frac{t}{\tau}\right] \end{aligned} \quad (1)$$

(Greenspan, 1969) where  $t$  is time after the incremental change in rotation rate. This behaviour holds for low Ekman and Rossby numbers ( $Ro = \Delta\Omega/\Omega$ ) and has been verified both experimentally (Warn-Varnas et al., 1978) and numerically (Duck and Foster, 2001).

### 4. Experimental measurements of effective viscosity

The results of a typical experiment are shown in Fig. 2. The colour contour plot in Fig. 2a shows how  $u$  varies as a function of the distance,  $d$ , along the ultrasonic beam. Fig. 2b presents slices at specific  $d$  values of the results displayed in Fig. 2a. Note that the velocities increase exponentially in time towards the new spin-up value. We invert these velocity measurements in order to retrieve the characteristic spin-up time,  $\tau$ , as a function of position within the sphere.

#### 4.1. Non-convective experiments

Fig. 3 shows experimental measurements of  $\tau$  made during spin-up from 300 to 340 rpm and plotted versus cylindrical radius. Fig. 3 also contains theoretical  $\tau$  profiles produced using Eq. (1). Using the averaged rotation rate ( $\Omega + \Delta\Omega/2$ ) of the container in Eq. (1), we carry out least-squares inversions of our spin-up measurements to determine the effective viscosity of the fluid. In the isothermal (non-convecting,  $T_1 = T_2 = 16^\circ\text{C}$ ) case, shown with red lines in Fig. 3, the effective viscosity matches the value of the molecular viscosity to within 2%. Thus we are able to recover the molecular viscosity characterising viscous coupling between the fluid and the shell in experiments where convective flow is not present. This test has been done successfully for different isothermal temperature values (i.e. for varying values of the viscosity (Lide, 1995)) within the following parameter

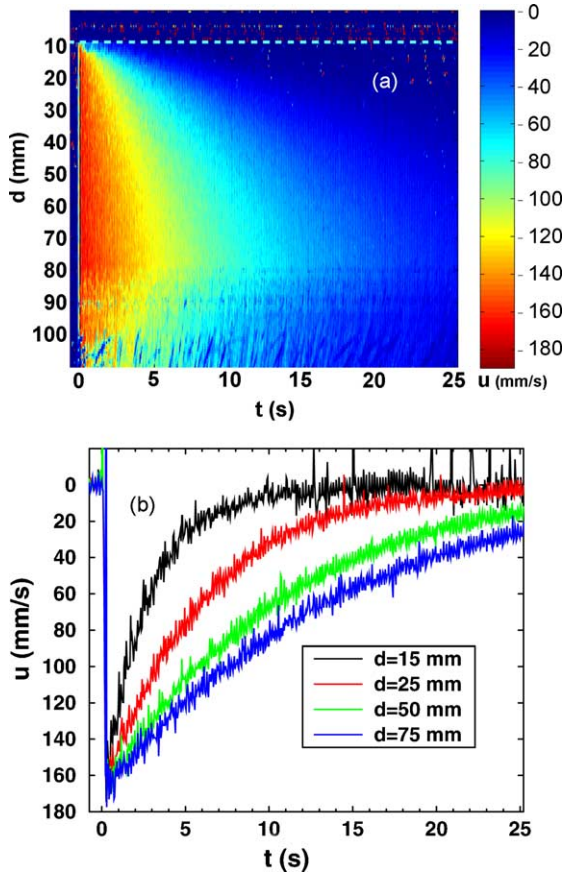


Fig. 2. Measured velocity  $u$  along  $d$  for spin-up occurring at  $t = 0$ ,  $E = 2.7 \times 10^{-6}$ ;  $Ro = 0.13$ ,  $T_1 = T_2 = 16^\circ\text{C}$ : (a) colour contour plot of measured velocity as a function of time,  $t$ , and distance,  $d$ , along the ultrasonic beam. The white dashed line shows the distance at which the ultrasonic beam enters the fluid. (b) Time-series of measured velocity,  $u$ , at four different values for  $d$ .

range  $16^\circ\text{C} < T_1 = T_2 < 35^\circ\text{C}$ ,  $0.06 < Ro < 0.13$ ,  $2.5 \times 10^{-6} < E < 6.7 \times 10^{-6}$ . In all these isothermal cases, the inversion always retrieves the molecular viscosity within a maximum of 2% error.

#### 4.2. Convective experiments

In the presence of turbulent thermal convection, we observe that the measured velocity profiles still follow the radial dependence predicted by Eq. (1). Thus, it is possible to use the same basic procedure to obtain the effective viscosity of the turbulent fluid. Because the

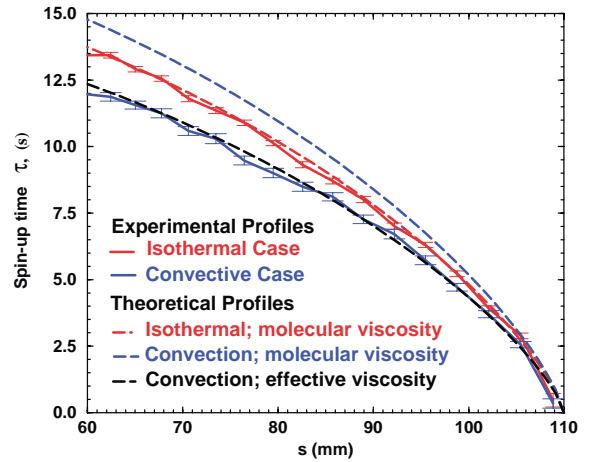


Fig. 3. Profiles of spin-up time-scale,  $\tau$ , plotted versus cylindrical radius,  $s$ . In all cases shown  $\Omega = 300$  rpm and  $\Delta\Omega = 40$  rpm. Experimental profiles are shown as solid lines with error bars: in red, isothermal spin-up ( $T_1 = T_2 = 16^\circ\text{C}$ ); in blue: spin-up in presence of thermal convection ( $T_1 = 4.0^\circ\text{C}$ ;  $T_2 = 30.0^\circ\text{C}$ ;  $T_{\text{averaged}} = 21.3^\circ\text{C}$ ;  $Ra = 1.0 \times 10^9$ ). Dashed lines show profiles predicted using Eq. (1), a rotation rate of  $(\Omega + \Delta\Omega)/2 = 320$  rpm, and various fluid viscosity values. The black dashed line shows the profile for the best-fitting value of the viscosity from a least-squares inversion of the spin-up measurements from the convective case. This effective viscosity is 43% greater than the molecular viscosity of the fluid at the averaged temperature (blue dashed line).

viscosity of the fluid changes with temperature, which varies through the shell in the convection experiments, we compute the spatially-averaged temperature of the fluid in order to proceed. From numerical simulations of the isotherms in the experimental geometry, the average temperature of the fluid is found to vary as  $T_{\text{averaged}} = T_1 + 1.33(T_2 - T_1)/2$ . In the convective spin-up experiment shown in Fig. 3 as an example, an effective viscosity 43% greater (black, short-dashed line) than the molecular viscosity (blue, long-dashed line) is needed to explain the shorter spin-up time in comparison to the non-convective case.

Table 1 is a compilation of the performed convective spin-up experiments that gives the experimental parameters and the corresponding turbulent, effective viscosities deduced from experiments. Note that by using the results of the previous experimental study by Aubert et al. (2001) carried out in the same apparatus, we were able to precisely determine the ratio  $Ra/Ra_C$ , the ratio of the Rayleigh number over the critical Rayleigh number for each experiment. The

Table 1  
Parameters and results of the convective experiments

$\Omega$ (rpm)	$(\Omega + \Delta\Omega)$ (rpm)	$T_1$ (°C)	$T_2$ (°C)	$Ra/Ra_C$	$\nu_{\text{eff}}/\nu$
300	340	22	34	24.1	1.16
300	340	12	33	40.9	1.36
*300	340	4	30	50.7	1.43
360	400	22	36	29.2	1.18
360	400	12	36	52.0	1.35
360	400	4	36	73.4	1.54
500	540	22	38	40.8	1.19
500	540	12	38	68.1	1.40
500	540	4	32	78.2	1.49

$\Omega$  is the initial angular velocity in revolutions per min,  $\Omega + \Delta\Omega$  the angular velocity right after the spin-up,  $T_1$  the temperature of the inner cylinder,  $T_2$  the temperature of the outer shell, the ratio  $Ra/Ra_C$  is computed from Aubert et al. (2001) and the ratio  $\nu_{\text{eff}}/\nu$  is obtained from the inversion as described in Fig. 3. Error bars on the viscosity ratio values  $\nu_{\text{eff}}/\nu$ , are approximately 10%. Note that the third experiment (with a star) is the experiment of Fig. 3.

experimental data in Table 1 show clearly an increase of the effective viscosity with the turbulence of the flow: increasing the vigour of the convection (increase of the ratio  $Ra/Ra_C$ ) with a constant rotation rate (spin-up from 300 to 340, 360 to 400 or from 500 to 540 rpm) increases the turbulent viscosity needed to explain a shorter spin-up as illustrated in Fig. 3. Note that Lathrop et al. (1992) found a turbulent viscosity scaling-law by measuring the motor torque in a suite of Taylor–Couette experiments. There the turbulent viscosity was deduced through a globally-integrated boundary effect. Here we invert for the turbulent viscosity from non-invasive, local measurements of the interior flow field.

## 5. Conclusions and discussion

Two main conclusions are reached from our experiments. First, the spin-up process between the fluid and a spherical shell is more efficient in the presence of thermal convection, leading to a faster spin-up time in comparison to isothermal cases. Second, the effective viscous coupling, controlled by the turbulent fluid viscosity in the Ekman boundary layer, clearly increases (Table 1) with the vigour of the convection in the bulk of the fluid flow. The physical mechanism leading to a more efficient viscous coupling in presence of turbu-

lence will need to be fully investigated and understood with future experimental, theoretical and numerical studies. These studies should focus on topics, such as the effect of differing fluid properties (thermal diffusivities for example). Experimental studies with high levels of mechanically-forced turbulence may also improve our understanding of this phenomenon. Numerical (and theoretical) studies should prove ideal for probing how the Reynolds stresses cause enhanced momentum transfer as function of Rayleigh and Ekman numbers.

Although caution must presently be taken in directly applying our experimental results to planetary cores, our experimental results qualitatively suggest that a larger effective viscosity value than the molecular one should be used in modelling core-mantle boundary dynamics on Earth (Gubbins and Roberts, 1987; Jault et al., 1988) and the terrestrial planets (Correia and Laskar, 2001). As an immediate consequence, the Ekman boundary layer may be increased in thickness and the viscous torque at the Earth’s core-mantle boundary will increase as well, possibly even becoming as large as estimated topographic or electromagnetic torques. Viscous phenomena such as damping of oscillatory modes (Zatman and Bloxham, 1997), planetary nutations, librations and interior dissipation processes (Williams et al., 2001) may be strongly affected by convective turbulence in core fluids. Furthermore, our results, which formally shed light only on boundary layer processes, may suggest that the present generation of large-scale, high viscosity, numerical geodynamo models are more similar to the real Earth than presumed. And perhaps this similarity explains why such models are working so surprisingly well.

## Acknowledgements

This research was supported by the program “Intérieur de la Terre” of CNRS/INSU and by the Université Joseph Fourier. J.A. received financial support from NASA PP and G grants (#NAG5-4007 and #NAG5-10165) and from a NSF-CNRS travel grant. We thank B. Buffett and an anonymous reviewer for useful comments to improve the manuscript. P.C. would like to thank P. Olson, I. Sumita and J. Aubert for fruitful discussions during previous attempts to measure turbulent viscosity.

## References

- Aubert, J., Brito, D., Nataf, H.-C., Cardin, P., Masson, J.-P., 2001. A systematic experimental study of rapidly rotating spherical convection in water and liquid gallium. *Phys. Earth Planet Int.* 128, 51–74.
- Brito, D., Nataf, H.-C., Cardin, P., Aubert, J., Masson, J.-P., 2001. Ultrasonic Doppler velocimetry in liquid gallium. *Exp. Fluids* 31, 653–663.
- Buffett, B., 1992. Constraints on magnetic energy and mantle conductivity from the forced nutations of the Earth. *J. Geophys. Res.* 97, 19581–19597.
- Busse, F., Carrigan, C., 1976. Laboratory simulation of thermal convection in rotating planets and stars. *Science* 191, 81–83.
- Cardin, P., Olson, P., 1994. Chaotic thermal convection in a rapidly rotating spherical shell: consequences for flow in the outer core. *Phys. Earth Planet Int.* 82, 259.
- Correia, A., Laskar, J., 2001. The four final rotation states of Venus. *Nature* 411, 767–770.
- De Wijs, G., Kresse, G., Vocadlo, L., Dobson, D., Alfè, D., Gillan, M., Price, G., 1998. The viscosity of liquid iron under Earth's core conditions. *Nature* 392, 805–807.
- Dobson, D.P., Crichton, W.A., Vocadlo, L., Jones, A.P., Wang, Y., Uchida, V., Rivers, M., Sutton, S., Brodholt, J.P., 2000. In situ measurement of viscosity of liquids in the Fe–FeS system at high pressures and temperatures. *Am. Mineral* 85, 1838–1842.
- Duck, P., Foster, M., 2001. Spin-up of homogeneous and stratified fluids. *Ann. Rev. Fluid Mech.* 33, 231–263.
- Frish, U., 1995. *Turbulence*. Cambridge University Press, Cambridge.
- Glatzmaier, G., Roberts, P., 1995. A three-dimensional self-consistent computer simulation of a geomagnetic field reversal. *Nature* 377, 203–209.
- Glatzmaier, G., 2002. Geodynamo simulations—How realistic are they? *Annu. Rev. Earth Planet Sci.* 30, 237–257.
- Greenspan, H., 1969. *The Theory of Rotating Fluids*. Cambridge University Press, Cambridge.
- Gubbins, D., Roberts, P., 1987. In: J. Jacobs (Eds.), *Geomagnetism*. Academic Press, London.
- Hulot, G., Eymin, C., Langlais, B., Mandea, M., Olsen, N., 2002. Small-scale structure of the geodynamo inferred from Oersted and Magsat satellite data. *Nature* 416, 630–633.
- Jault, D., Gire, C., Le Mouél, J.-L., 1988. Westward drift, core motions and exchanges of angular momentum between core and mantle. *Nature* 333, 353–356.
- Jones, C., 2000. Convection-driven geodynamo models. *Phil. Trans. R. Soc. London A* 358, 873–897.
- Kuang, W., Bloxham, J., 1997. A numerical dynamo model in an Earth-like dynamical regime. *Nature* 389, 371–374.
- Lathrop, D., Fineberg, J., Swinney, H., 1992. Transition to shear-driven turbulence in Couette–Taylor flow. *Phys. Rev. A* 46, 6390–6405.
- Lide, D., 1995. *Handbook of Chemistry and Physics*. CRC Press, Boca Raton.
- Olson, P., Christensen, U., Glatzmaier, G., 1999. Numerical modeling of the geodynamo: Mechanisms of field generation and equilibration. *J. Geophys. Res.* 104, 10383–10404.
- Pedlosky, J., 1987. *Geophysical Fluid dynamics*. Springer, New-York.
- Poirier, J.P., 1988. Transport properties of liquid metals and viscosity of the Earth's core. *Geophys. J.* 92, 99–105.
- Prandtl, L., 1925. Bericht ueber Untersuchungen zur ausgebildeten Turbulenz. *ZAMM* 5, 136–139.
- Rutter, M.D., Secco, R.A., Uchida, T., Liu, H., Wang, Y., Rivers, M.L., Sutton, S.R., 2002. Towards evaluating the viscosity of the Earth's outer core: an experimental high pressure study of liquid Fe-S (8.5 wt.%S). *Geophys. Res. Lett.* 29 (8), 58.1–58.4.
- Secco, R., 1995. T. Arhens (Ed.), *Mineral Physics and Crystallography: A Handbook of Physical Constants*. American Geophysical Union, Washington.
- Smylie, D., 1999. Viscosity near Earth's solid inner core. *Science* 284, 461–463.
- Sumita, I., Olson, P., 1999. A laboratory model for the convection in the Earth's core driven by a thermally heterogeneous mantle. *Science* 286, 1547–1549.
- Warn-Varnas, A., Fowles, W., Piacsek, S., Lee, S., 1978. Numerical solutions and laser-Doppler measurements of spin-up. *J. Fluid Mech.* 85, 609–639.
- Williams, J., Boggs, D., Yoder, C., Ratcliff, J., Dickey, J., 2001. Lunar rotational dissipation in solid body and molten core. *J. Geophys. Res. Planets* 106, 27933–27968.
- Zatman, S., Bloxham, J., 1997. Torsional oscillations and the magnetic field within the Earth's core. *Nature* 388, 760–763.